



Multicentric development and evaluation of ^{18}F -FDG PET/CT and MRI radiomics models to predict para-aortic lymph node involvement in locally advanced cervical cancer

François Lucia^{1,2,3} · Vincent Bourbonne^{1,2} · Clémence Pleyers⁴ · Pierre-François Dupré⁵ · Omar Miranda¹ · Dimitris Visvikis² · Olivier Pradier^{1,2} · Ronan Abgral^{6,7} · Augustin Mervoyer⁸ · Jean-Marc Classe⁹ · Caroline Rousseau^{10,11} · Wim Vos¹² · Johanne Hermesse⁴ · Christine Gennigens¹³ · Marjolein De Cuypere¹⁴ · Frédéric Kridelka¹⁴ · Ulrike Schick^{1,2} · Mathieu Hatt² · Roland Hustinx³ · Pierre Lovinfosse³

Received: 4 November 2022 / Accepted: 27 February 2023

© The Author(s), under exclusive licence to Springer-Verlag GmbH Germany, part of Springer Nature 2023

Abstract

Purpose To develop machine learning models to predict para-aortic lymph node (PALN) involvement in patients with locally advanced cervical cancer (LACC) before chemoradiotherapy (CRT) using ^{18}F -FDG PET/CT and MRI radiomics combined with clinical parameters.

Methods We retrospectively collected 178 patients (60% for training and 40% for testing) in 2 centers and 61 patients corresponding to 2 further external testing cohorts with LACC between 2010 to 2022 and who had undergone pretreatment analog or digital ^{18}F -FDG PET/CT, pelvic MRI and surgical PALN staging. Only primary tumor volumes were delineated. Radiomics features were extracted using the Radiomics toolbox®. The ComBat harmonization method was applied to reduce the batch effect between centers. Different prediction models were trained using a neural network approach with either clinical, radiomics or combined models. They were then evaluated on the testing and external validation sets and compared.

Results In the training set ($n = 102$), the clinical model achieved a good prediction of the risk of PALN involvement with a C-statistic of 0.80 (95% CI 0.71, 0.87). However, it performed in the testing ($n = 76$) and external testing sets ($n = 30$ and $n = 31$) with C-statistics of only 0.57 to 0.67 (95% CI 0.36, 0.83). The ComBat-radiomic (GLDZM_HISDE_PET_FBN64 and Shape_maxDiameter2D3_PET_FBW0.25) and ComBat-combined (FIGO 2018 and same radiomics features) models achieved very high predictive ability in the training set and both models kept the same performance in the testing sets, with C-statistics from 0.88 to 0.96 (95% CI 0.76, 1.00) and 0.85 to 0.92 (95% CI 0.75, 0.99), respectively.

Conclusions Radiomic features extracted from pre-CRT analog and digital ^{18}F -FDG PET/CT outperform clinical parameters in the decision to perform a para-aortic node staging or an extended field irradiation to PALN. Prospective validation of our models should now be carried out.

Keywords Radiomics · Cervical cancer · Para-aortic lymph node · ^{18}F -FDG PET/CT · Digital ^{18}F -FDG PET/CT · MRI

This article is part of the Topical Collection on Advanced Image Analyses (Radiomics and Artificial Intelligence)

✉ François Lucia
francois.lucia@chu-brest.fr

Extended author information available on the last page of the article

Introduction

The standard of care for locally advanced cervical cancer (LACC) (FIGO 2018 stage $\geq\text{IB3}$), is based on radiation therapy (RT) combined with concurrent chemotherapy (40 mg/m² cisplatin or carboplatin AUC2 weekly) followed by Image Guided Adaptive Brachytherapy (IGABT) [1]. Lymph node involvement (LNI) is a major prognostic factor in LACC and patients with positive para-aortic lymph nodes (PALN) will be treated with an extended field of irradiation to the para-aortic region [1]. However, irradiation of these

nodes is associated with a significant increase in morbidity, with a risk of grade 3 and 4 toxicity in 15% of the patients [2]. Thus, it is essential to select the patients who are really likely to benefit from PALN irradiation. Current recommendations are to first perform a PALN staging by ^{18}F -FDG PET/CT completed by a PALN dissection for patients without PALN involvement (PALNI) on ^{18}F -FDG PET/CT [1]. Indeed, the false-negative (FN) rate on ^{18}F -FDG PET/CT is estimated at 12–20% [3, 4]. However, this surgical procedure is associated with high intraoperative and postoperative morbidity that may delay the initiation of definitive chemoradiotherapy [5]. Moreover, studies have reported conflicting results of surgical staging on recurrence-free survival and overall survival [6, 7]. In this context, the question of surgical de-escalation has emerged [6]. Thus, development of predictive models using non-invasive tools seems necessary to predict PALNI and to assist in decision making for extended field irradiation or surgical dissection. The FRANCOGYN group proposed a score based on 3 clinical parameters (MRI tumor size, the initial squamous cell carcinoma tumor marker (SCC), and pelvic LNI on ^{18}F -FDG PET/CT) to classify patients with a squamous cell carcinoma, the most common histological type (80–90% of cases) followed by adenocarcinoma (10–20% of cases) and rare histological types (<5%), into 3 risk groups for PALNI: low, intermediate, and high risk [8]. They suggested that low-risk patients do not necessitate surgical staging and extended-field irradiation, whereas other patients could benefit from surgical staging and extended-field irradiation for those with PA nodal extension on final histology.

Quantitative analysis of medical images such as ^{18}F -FDG PET/CT and MRI have been shown to reflect tumor heterogeneity and several predictive and prognostic models, including for LACC have been developed [9, 10]. Some models have focused on the prediction of pelvic LNI before surgery in early-stage cervical cancer [11–15]. However, to the best of our knowledge, the added value of radiomic features on the prediction of PALNI before CRT to avoid staging dissection has never been reported before. Machine learning (ML) methods, in particular artificial neural networks (ANN) [16, 17], allows to build predictive models by combining parameters using a flexible nonlinear relationship [18]. In addition, the integration of a new type of detectors has allowed the development of so-called “digital” PET/CT scanners, replacing the classical “analog” PET/CT. Recent studies have shown an improvement of image quality and lesion detectability with a digital PET/CT system [19]. Thus, digital PET/CT will likely gradually replace analog PET/CT, making it necessary to evaluate radiomic models on this new generation of PET/CT.

The aim of this study was to develop ML models to predict PALNI in patients with LACC using ^{18}F -FDG PET/CT and/or MRI radiomics features from the primary tumor volume, combined (or not) with clinical parameters.

Methods

Patients' information

Patients with a LACC (FIGO 2018 stage IB3-IVA) who underwent a PALN dissection without PALNI on ^{18}F -FDG PET/CT at three institutions (University Hospital (CHU) of Brest in France, ICO St. Herblain in France, and University Hospital of Liège in Belgium) between 2010 and 2022 (2012–2022 at the CHU of Brest, 2015–2016 at the ICO and 2010–2020 at the CHU of Liège) were retrospectively considered (Table 1). All patients underwent a ^{18}F -FDG PET/CT and a pelvic MRI, both at diagnosis. Clinical and pathological data included age and date of diagnosis, histology, FIGO stage (2009 and 2018 before surgical staging), presence of positive pelvic LN on PET/CT (according to the report of the nuclear physician), tumor size as measured on MRI (according to the report of the radiologist). Of the 263 eligible patients, 24 patients were not included because of neoadjuvant chemotherapy ($n=10$) or surgical staging not feasible during surgery ($n=14$) (Fig. 1). Finally, a total of 93 patients were recruited at the CHU of Brest, 62 patients who had an analog PET/CT (2012–2018) and 31 patients who had a digital PET/CT (2019–2022) and were included after model building for external testing on digital PET/CT, 30 at the ICO St Herblain and 116 at the CHU of Liège.

Surgical procedure

The surgery was performed by surgeons specialized in pelvic gynecological oncology, with more than 10 years of experience. After excluding peritoneal invasion, PALN dissection removed all lymphatic tissue from the aorta, aortocaval space, and vena cava using a minimally invasive surgical approach. The caudal limit of surgery was the bifurcation of the external and internal iliac artery. Cranially, dissection was performed to the inferior mesenteric artery or the left renal vein at its crossing with the abdominal aorta. If a macroscopically suspicious node was observed, an elective para-aortic adenectomy was performed and subjected to frozen section. PALN dissection was continued only if the frozen section was negative for metastases. Pelvic lymphadenectomy was not routinely performed. Involved PALN included both macroscopic and microscopic metastases.

PET/CT imaging

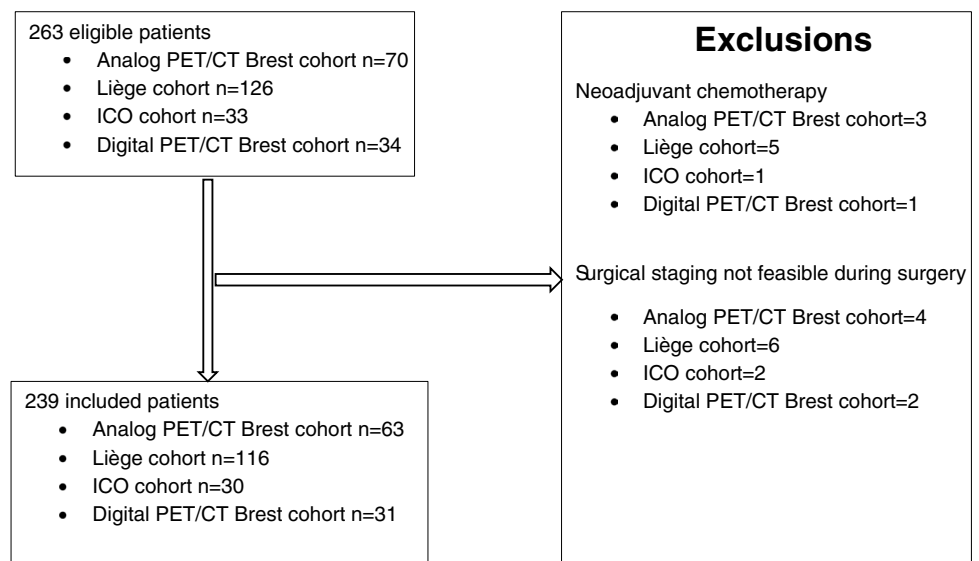
PET/CT studies were performed with 3 types of scanners and 4 types of acquisition. In the CHU of Brest (between 2012 and 2018) and ICO St. Herblain studies were performed in both sites with a Siemens Biograph mCT, with

Table 1 Patients' characteristics

	Training		Testing		ICO		Digital PET/CT		Difference (<i>p</i> value)
	<i>n</i> =102	%	<i>n</i> =76	%	<i>n</i> =30	%	<i>n</i> =31	%	
Age median (range)	51 (29–79)		52 (26–77)		46 (23–73)		51 (29–70)		0.64
Tumor size on MRI	4.8 (2.6–11.4)		5.1 (1.5–9.2)		4.6 (2.0–11.1)		4.8 (2.9–11.3)		0.81
FIGO stage									0.47
IB3	11	11	8	10	2	7	0	0	
IIA	3	3	1	1	3	10	1	3	
IIB	33	32	18	24	11	37	7	23	
IIIA	1	1	0	0	1	3	0	0	
IIIB	5	5	2	3	0	0	1	3	
IIIC1	44	43	44	58	12	40	19	61	
IVA	5	5	3	4	1	3	3	10	
Histology									0.42
Squamous cell carcinoma	92	90	67	88	27	90	28	90	
Adenocarcinoma	6	6	5	7	3	10	3	10	
Adenosquamous carcinoma	4	4	4	5	0	0	0	0	
Pelvic lymph node involvement									0.26
Uninvolved	57	56	32	42	17	57	11	35	
Involved	45	44	44	58	13	43	20	65	
Para-aortic lymph node involvement									0.57
Uninvolved	84	82	60	79	24	80	26	84	
Involved	18	18	16	21	6	20	5	16	

Abbreviations: FIGO=International Federation of Gynecology and Obstetrics, MRI=magnetic resonance imaging

Fig. 1 Flowchart of patient selection at the three recruiting institutions (training and testing and external evaluation sets)



however some differences in the acquisition, in the CHU of Brest (between 2019 and 2022), studies were acquired using a Siemens digital Biograph Vision 600, in the CHU of Liège, studies were acquired using a Philips Gemini TF or BB (supplemental data A, Table S1).

MRI imaging

All patients underwent pretreatment 1.5 T MRI scans including T2-weighted (T2W), and the ADC map derived from diffusion-weighted imaging (DWI) (detailed information for

MRI scanners and associated parameters in supplemental data A, Table S1).

Tumor volume delineation

^{18}F -FDG PET exams were imported into a MIM workstation (MIM Software®, Cleveland, OH, USA). Segmentation of the 3D primary tumor volume was semi-automatically performed by an experienced radiation oncologist (F.L.) using a gradient-based method (PET-Edge®) [20].

The primary tumor was also delineated on (i) the ADC map derived from DWI-MRI and (ii) T2W-MRI. Each sequence was segmented independently because of anatomical changes between each sequence acquisition, using a previously validated semi-automatic approach exploiting 3D Slicer® and the Growcut algorithm [21].

Radiomic features characterization of the tumor volumes

Two hundred and seventeen features were extracted from the segmented volumes in each image modality using the Radiomics toolbox® (Oncoradiomics SA, Liège, Belgium) (detailed description of the features in supplemental data B). For those standardized by the IBSI (Imaging biomarkers standardization initiative), the implementation follows the IBSI benchmark [22]. Before calculation, radiomic features were extracted after $2 \times 2 \times 2 \text{ mm}^3$ spatial resampling for all PET images, and $1 \times 1 \times 1 \text{ mm}^3$ spatial resampling for MRI using a cubic spline interpolation. For the calculation of the texture matrix-based features, image intensities were discretized using two different methods according to IBSI recommendations: fixed bin number (FBN, using 32 and 64 bins) and fixed bin width (FBW 0.25 SUV and 10 for MRI ADC as the ADC map is quantitative, but not on the T2 MRI) [22]. As a result, 1435 radiomics features (198×3 (FBN and FBW value) + 19 = 613 for PET/CT and (153×2 (FBN value) + 19) \times 2 (T2W and ADC) and 172 (FBW for MRI ADC) = 822 for MRI) were available for each patient.

Modelling strategy

In addition to the radiomic features, data also included 6 clinical parameters, i.e., FIGO stage 2009 and 2018 before surgical staging, histological types (squamous cell carcinoma, adenocarcinoma, or adenosquamous carcinoma), age, presence of lymph node pelvic metastasis on ^{18}F -FDG PET/CT, and size on MRI measured by radiologist.

We considered the combination of the Brest analog PET/CT (2012–2018) and Liège cohorts (Brest-Liège cohort) and split it into a training set of 102 patients (approximately 60% of the total) and a first testing set of 76 patients (approximately 40% of the total). The ICO and

Brest digital PET/CT (2019–2022) cohorts were used for further external evaluation (Figure S1, supplemental data A).

We tested different approaches for model training and testing (Supplemental data C). Indeed, different combinations were tried to find the best compromise to have a training dataset with enough events (para-aortic lymph node involvement) and avoid overfitting.

A feature set reduction was performed (training data set only) to reduce the high number of radiomic features and to reduce the risk of overfitting (Supplemental data C). Radiomic and Clinical features were entered as input into a Neural Network Approach (Multilayer Perceptron Network, SPSS Modeler v18.3®) with the Bootstrap Aggregating tool to improve stability and robustness [17]. Before each model was built, correction for unbalanced data was performed using the Synthetic Minority Over-sampling Technique-Nominal Continuous (SMOTE-NC). We trained 3 models: clinical, radiomic, combined. The trained models were then evaluated on the testing sets.

Given the number of combinations of PET/CT and MRI scanner models and acquisition/reconstruction settings present in our multicentric dataset, the ComBat a posteriori statistical harmonization method was used [23]. It was applied before feature set selection for each approach and model building, thus creating 2 additional models: ComBat radiomic, ComBat combined. As a result, 5 models were developed and evaluated. Full description of the modelling strategy is available in the supplemental data.

Each model was evaluated using the Area Under the Curve (AUC) along with the C-statistic, as well as the Balanced Accuracy (Bacc) and associated sensitivity (Se), specificity (Sp), number of FN and false-positive (FP) after setting a threshold on the training cohort. Importance of each feature in each model was also reported. Decision curve analysis (DCA) was also used for inter-model comparison.

We also compared our best models to the available nomogram of FRANCOGYN group. This score applies only to squamous cell carcinoma. Moreover, we only had the initial SCC for patients from analog and digital PET/CT Brest cohorts. Thus, we compared the models only on patients from Brest with a squamous cell carcinoma.

All the statistical analyses were performed using SPSS® (Statistics and Modeler version 24.0 and 18.3, IBM, Armonk, NY) and MedCalc® (version 15.8, MedCalc Software bvba, Ostend, Belgium).

Ethics committee

The study was approved by the different hospital ethical committees.

Results

Among 239 patients who underwent PALN dissection, PALNI was found in 45 patients (19%), 12 patients in the analog PET/CT cohort of the CHU of Brest (19%), 5 patients in the digital PET/CT cohort of the CHU of Brest (16%), 6 patients in the ICO cohort (20%), and 22 patients at the CHU of Liège (19%).

Models from the Brest-Liège cohort

The cohort was randomly divided into a training set ($n = 102$) and a testing set ($n = 76$) who were globally comparable in terms of PALNI, with 18/102 (18%) and 16/76 (21%), respectively ($p = 0.76$). For radiomic features and before statistical harmonization, reduction of the feature set on the training set resulted in a preselection of 151 radiomic features with an AUC ≥ 0.70 , from PET-CT and the T2 sequence. No radiomic features of the ADC map was selected. At the second step (Spearman rank correlation coefficient), only eight radiomic features showed intra-correlation levels below 0.7 and were subsequently used to train the models.

The best clinical model combined 3 features (FIGO stage 2018, MRI tumor size and pelvic lymph node on PET/CT). The best radiomic and combined models were based on 3 (GLDZM_LDE_PET_FBW0.25, Shape_maxDiameter2D3_PET_FBW0.25, and NGLDM_SM2_PET_FBW0.25) and 4 (same radiomics features and FIGO stage 2018) variables, respectively, among which the most important one was NGLDM_SM2_PET_FBW0.25 (contribution of 65.3% and 53.7%, respectively).

After ComBat harmonization, the best ComBat-radiomic and the ComBat-combined models consisted in the association of 2 (GLDZM_HISDE_PET_FBN64 and Shape_maxDiameter2D3_PET_FBW0.25) and 3 (the same 2 radiomic features and the FIGO stage 2018) variables, respectively, and the most important feature was GLDZM_HISDE_PET_FBN64 (71.1% and 67.4%, respectively).

Composition of each model is available in Supplemental data A, Table S2.

In the training set ($n = 102$), the clinical model achieved a high prediction of the risk of LNI with an AUC of 0.86 (95% CI 0.78, 0.93) and a C-statistic of 0.80 (95% CI 0.71, 0.87) with a cut-off of 26%. The radiomic and combined models achieved a very good prediction of the risk of PALNI with an AUC of 0.88 (95% CI 0.80, 0.94) and a C-statistic of 0.83 (95% CI 0.74, 0.90) with a cut-off of 14% and AUC of 0.90 (95% CI 0.83, 0.97) and a C-statistic of 0.81 (95% CI 0.72, 0.88) with a cut-off of 11%, respectively. The ComBat-radiomic and ComBat-combined

models achieved higher performance with an AUC of 0.95 (95% CI 0.88, 0.99) and a C-statistic of 0.94 (95% CI 0.87, 0.97) with a cut-off of 24% and AUC of 0.90 (95% CI 0.83, 0.97) and a C-statistic of 0.82 (95% CI 0.73, 0.89) with a cut-off of 10%, respectively (Table 2).

In the testing ($n = 76$) and external testing sets ($n = 30$ and $n = 31$), the clinical model predicted the risk of PALNI with much lower AUCs of 0.62 to 0.69 (95% CI 0.48, 0.85) and C-statistics of 0.57 to 0.67 (95% CI 0.36, 0.83) with a cut-off of 26%. The ComBat-radiomic and ComBat-combined models were the most efficient models with AUCs of 0.90 to 0.96 (95% CI 0.81, 1.00) for both of them and C-statistics of 0.88 to 0.96 (95% CI 0.76, 1.00) and 0.85 to 0.92 (95% CI 0.75, 0.99), respectively, with a cut-off of 24% and 10%, respectively. In comparison, the radiomic and combined models resulted in lower (although still much higher than clinical only) C-statistics of 0.78 to 0.81 (95% CI 0.59, 0.91) and 0.78 to 0.90 (95% CI 0.59, 0.95), respectively. The ComBat-radiomic and ComBat-combined models were associated with a risk of FN of 0.0% to 12.5% for both of them and a risk of FP of 3.8% to 16.7% and 15.4% to 23.3%, respectively, with their cut-off (Tables 3, 4, and 5).

We evaluate the time needed to apply our model in clinical routine (each step was timed, the reported time is for all 31 patients): data collection of PET/CT images and clinical parameters (120 min), segmentation (30 min), features extraction (10 min), ComBat harmonization (10 min), application for a model (10 min) for the 31 patients of the digital PET/CT Brest cohort.

For comparison, applied in the CHU of Brest cohort, with an analog PET/CT, the predictive score developed by the FRANCOGYN allowed a risk of FN of 30% (3/10) and a risk of FP of 63% (29/46) while the ComBat-radiomic and the ComBat-combined models, both developed in the Brest-Liège cohort (61% (34/56) patients in the training set and 39% (22/56) in the testing set, led to a risk of FN of 10% (1/10) for both of them and to a risk of FP of 28% (13/46) and 24% (11/46), respectively.

Applied in the CHU of Brest cohort with a digital PET/CT, the predictive score developed by the FRANCOGYN allowed a risk of FN of 40% (2/5) and a risk of FP of 65% (15/23) while the ComBat-radiomic and the ComBat-combined models expose to a risk of FN of 0% for both of them and to a risk of FP of 4% (1/23) and 17% (4/23), respectively.

Finally, DCA revealed that the ComBat models have a very good PALNI risk prediction (Fig. 2).

Simulations of the application of our models in clinical practice in the overall cohort and in comparison with the FRANCOGYN score in the CHU of Brest cohort are given in Figs. 3 and 4.

The results after normalization are available in the Supplemental data G.

Table 2 Brest-Liège cohort models in training set

Model	AUC	Model cut-off	C-statistic	Se	Sp	Bacc	Number of patients					
							Below the cut-off (no extended field irradiation)		Above the cut-off (extended field irradiation)			
							Total	Without PALNI	With PALNI	Total	Without PALNI	With PALNI
Clinical	0.86 [0.78–0.93]	26%	0.80 [0.71–0.87]	83.3 [58.6–96.4]	76.2 [65.7–84.8]	79.8 [62.2–90.6]	67	64	3	35	20	15
Radiomic	0.88 [0.80–0.94]	14%	0.83 [0.74–0.90]	100 [81.5–100]	66.7 [55.3–77.6]	83.4 [68.4–88.8]	56	56	0	46	28	18
Combined	0.90 [0.83–0.97]	11%	0.81 [0.72–0.88]	94.4 [69.4–100]	66.7 [55.3–77.6]	80.6 [62.4–88.8]	57	56	1	45	28	17
ComBat-radiomic	0.95 [0.88–0.99]	24%	0.94 [0.87–0.97]	100 [81.5–100]	86.9 [77.8–93.3]	93.5 [79.7–96.7]	73	73	0	29	11	18
ComBat-combined	0.90 [0.83–0.97]	10%	0.82 [0.73–0.89]	100 [81.5–100]	63.1 [51.9–73.4]	81.6 [66.7–86.7]	53	53	0	49	31	18

Data in brackets are 95% CIs

Abbreviations: AUC = area under the curve, Se = sensitivity, Sp = specificity, Bacc = balanced accuracy, PALNI = para-aortic lymph-node involvement

Table 3 Brest-Liège models in testing set

Model	AUC	Model cut-off	C-statistic	Se	Sp	Bacc	Number of patients					
							Below the cut-off (no extended field irradiation)		Above the cut-off (extended field irradiation)			
							Total	Without PALNI	With PALNI	Total	Without PALNI	With PALNI
Clinical	0.62 [0.50–0.73]	26%	0.58 [0.46–0.69]	43.7 [19.8–70.1]	71.2 [57.9–82.2]	57.5 [38.9–76.2]	51	42	9	25	18	7
Radiomic	0.85 [0.76–0.91]	18%	0.79 [0.69–0.88]	68.7 [55.8–80.4]	90 [67.4–95.6]	79.4 [61.6–88.0]	59	54	5	17	6	11
Combined	0.86 [0.77–0.92]	10%	0.78 [0.68–0.87]	68.7 [55.8–80.4]	86.7 [65.4–91.3]	78.4 [60.6–85.9]	57	52	5	19	8	11
ComBat-radiomic	0.90 [0.81–0.96]	24%	0.88 [0.78–0.94]	87.5 [61.7–98.4]	88.3 [77.4–95.2]	87.9 [69.6–96.8]	55	53	2	21	7	14
ComBat-combined	0.90 [0.81–0.96]	10%	0.85 [0.75–0.92]	93.7 [69.8–99.8]	76.7 [64.0–86.6]	85.2 [66.9–93.2]	47	46	1	29	14	15

Data in brackets are 95% CIs

Abbreviations: AUC = area under the curve, Se = sensitivity, Sp = specificity, Bacc = balanced accuracy, PALNI = para-aortic lymph-node involvement

Table 4 Brest-Liège models in ICO external evaluation set

Model	AUC	Model cut-off	C-statistic	Se	Sp	Bacc	Number of patients					
							Below the cut-off (no extended field irradiation)		Above the cut-off (extended field irradiation)			
							Total	Without PALNI	With PALNI	Total	Without PALNI	With PALNI
Clinical	0.69 [0.49–0.85]	26%	0.67 [0.47–0.83]	83.3 [35.9–99.6]	50.0 [29.1–70.9]	66.7 [32.5–85.3]	13	12	1	17	12	5
Radiomic	0.89 [0.75–0.94]	18%	0.81 [0.68–0.88]	66.7 [22.8–78.3]	95.8 [71.1–100]	81.3 [47.0–89.2]	25	23	2	5	1	4
Combined	0.91 [0.78–0.96]	10%	0.90 [0.77–0.95]	83.3 [35.9–99.6]	95.8 [71.1–100]	89.6 [53.5–99.8]	24	23	1	6	1	5
ComBat-radiomic	0.96 [0.82–0.99]	24%	0.92 [0.76–0.99]	100 [54.1–100]	83.3 [62.6–95.3]	91.7 [58.4–97.7]	20	20	0	10	4	6
ComBat-combined	0.96 [0.82–0.99]	10%	0.92 [0.76–0.99]	100 [54.1–100]	83.3 [62.6–95.3]	91.7 [58.4–97.7]	20	20	0	10	4	6

Data in brackets are 95% CIs

Abbreviations: AUC = area under the curve, Se = sensitivity, Sp = specificity, Bacc = balanced accuracy, PALNI = para-aortic lymph-node involvement

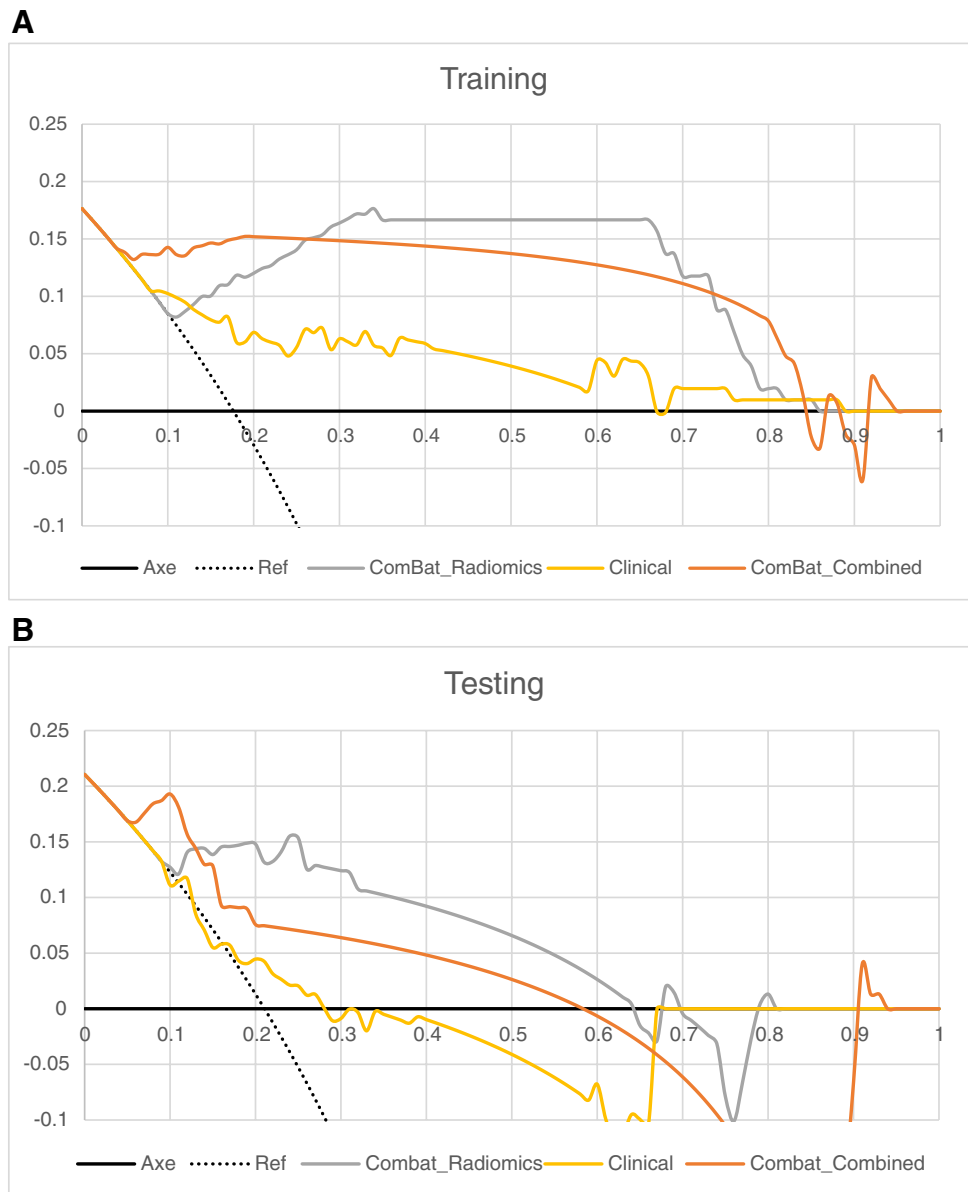
Table 5 Brest-Liège models in digital PET/CT external evaluation set

Model	AUC	Model cut-off	C-statistic	Se	Sp	Bacc	Number of patients					
							Below the cut-off (no extended field irradiation)		Above the cut-off (extended field irradiation)			
							Total	Without PALNI	With PALNI	Total	Without PALNI	With PALNI
Clinical	0.68 [0.48–0.84]	26%	0.57 [0.36–0.74]	80.0 [28.4–99.5]	29.2 [12.6–51.1]	54.6 [20.5–75.3]	8	7	1	21	17	4
Radiomic	0.84 [0.66–0.95]	18%	0.78 [0.59–0.91]	60.0 [14.7–94.7]	95.8 [78.9–99.9]	77.9 [46.8–97.3]	25	23	2	4	1	3
Combined	0.83 [0.65–0.94]	10%	0.78 [0.59–0.91]	60.0 [14.7–94.7]	95.8 [78.9–99.9]	77.9 [46.8–97.3]	25	23	2	4	1	3
ComBat-radiomic	0.96 [0.85–1.00]	24%	0.96 [0.85–1.00]	100 [47.8–100]	96.2 [80.4–99.9]	98.1 [64.1–100]	25	25	0	6	1	5
ComBat-combined	0.95 [0.84–1.00]	10%	0.92 [0.77–0.99]	100 [47.8–100]	84.6 [65.1–95.6]	92.3 [56.5–97.8]	22	22	0	9	4	5

Data in brackets are 95% CIs

Abbreviations: AUC = area under the curve, Se = sensitivity, Sp = specificity, Bacc = balanced accuracy, PALNI = para-aortic lymph-node involvement

Fig. 2 Decision curve analysis for the training (A) and testing (B) sets and external evaluation in the ICO (C) and digital PET/CT (D) cohorts



Models from the overall cohort, the Brest and Liège cohorts

These results are available in the Supplemental data D.

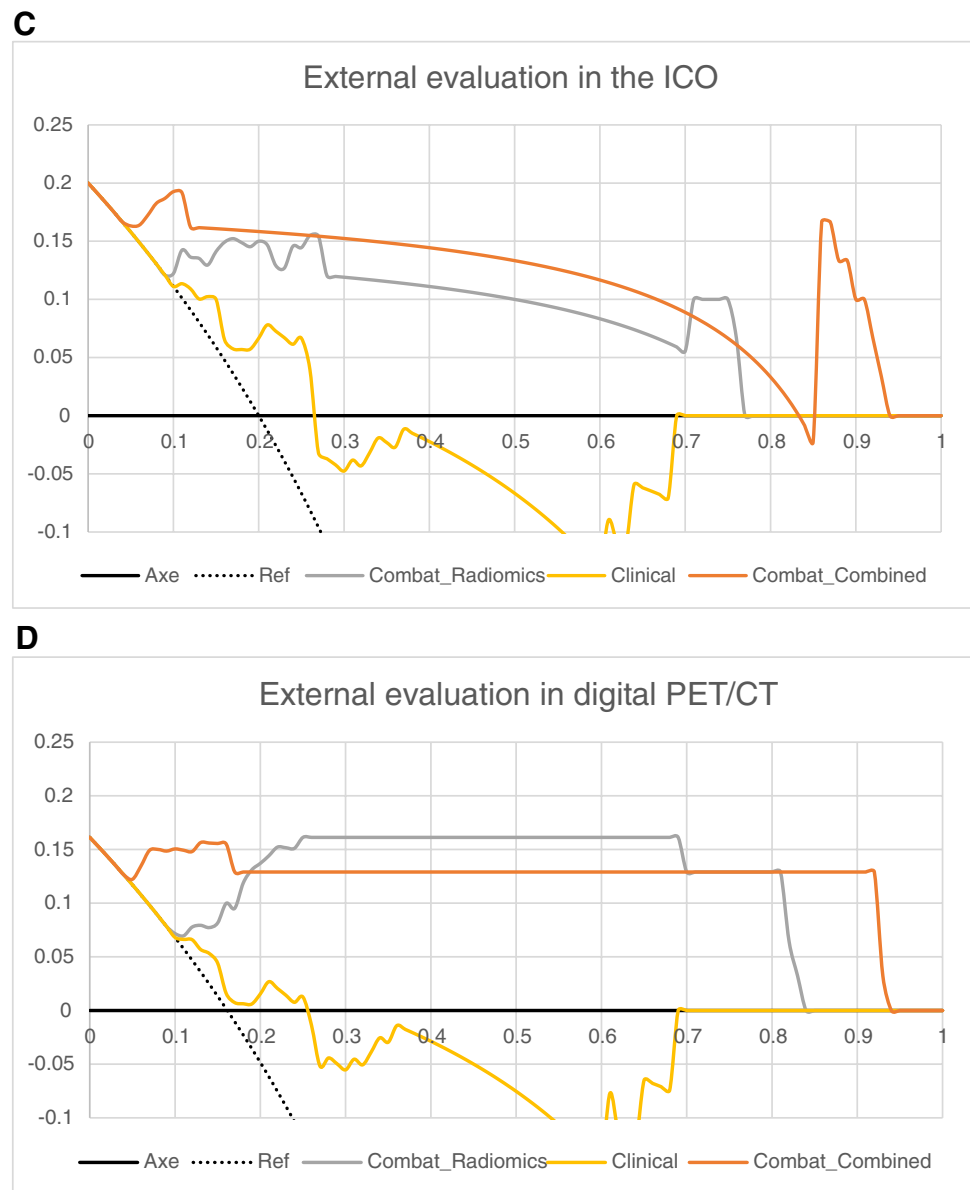
Discussion

Our study identified radiomics-based models built with machine learning that could be used in clinical practice to predict PALN invasion in LACC and guide clinicians in the planning of external beam fields of irradiation, without a surgical staging. These 2 models outperform the clinical model and the pre-existing models with a very good

sensitivity (from 88 to 100%) and a good specificity (from 77 to 96%).

The standard of care for patients with LACC prior to chemoradiotherapy includes a ^{18}F -FDG PET/CT and if no PALNI is found, surgical staging may be considered due to a FN rate (12 to 20%) with the ^{18}F -FDG PET/CT staging [3, 24, 25]. A recent study showed that with modern Time of Flight (TOF) ^{18}F -FDG PET/CT, the rate of FN remained important [26]. They showed that the FN rate was 8.5 to 10% with a FN rate of 3 to 5% in patients without pelvic nodal fixation but 15 to 17% in case of pelvic nodal fixation. In our study, the rates of FN are consistent with the literature with 19% in the overall cohort and 22% in patients with pelvic fixation. However, surgical de-escalation is increasingly debated [6, 24]. Indeed, some studies have found a benefit

Fig. 2 (continued)



on overall survival and recurrence-free survival of PALN dissection as a retrospective study conducted in 10 French centers comparing the therapeutic results of 377 patients who underwent staging and 270 who did not [7]. However, a recent report of the National Cancer DataBase showed that surgical staging had no impact on overall survival and recurrence-free survival [6]. Moreover, this surgical staging may induce perioperative complications that may delay concomitant chemoradiotherapy [27]. As a result, in our PET/CT digital cohort from Brest, the majority of patients had pelvic LNI, showing the change in practice in recent years where surgical staging is mainly proposed to these patients considered to have a higher risk of FN on ^{18}F -FDG PET/CT. However, the EBRT field depends on this PALN staging. Indeed, extended field irradiation is performed in case

of PALNI but lead to a significant increase in the rate of gastrointestinal toxicity [2]. Thus, it is essential to develop non-invasive tools for accurate PALNI evaluation.

Applying the score of the FRANCOGYN group [8] to our analog and digital PET/CT cohorts of squamous cell carcinoma in the CHU of Brest, among the 15 patients with involved PALN, 5 were in the low-risk group, i.e., 33% FN, and among the 69 patients without involved PALN, only 25 patients were in the low-risk group, i.e., 64% FP. Our 2 models allowed to drastically improve these performances with less FN patients, 7% for both of them and less FP, 20% and 22%, respectively. These 2 models are interesting because they do not require any additional examination, since the ^{18}F -FDG PET/CT is systematically performed during the assessment before CRT. Moreover, these are 2 simple

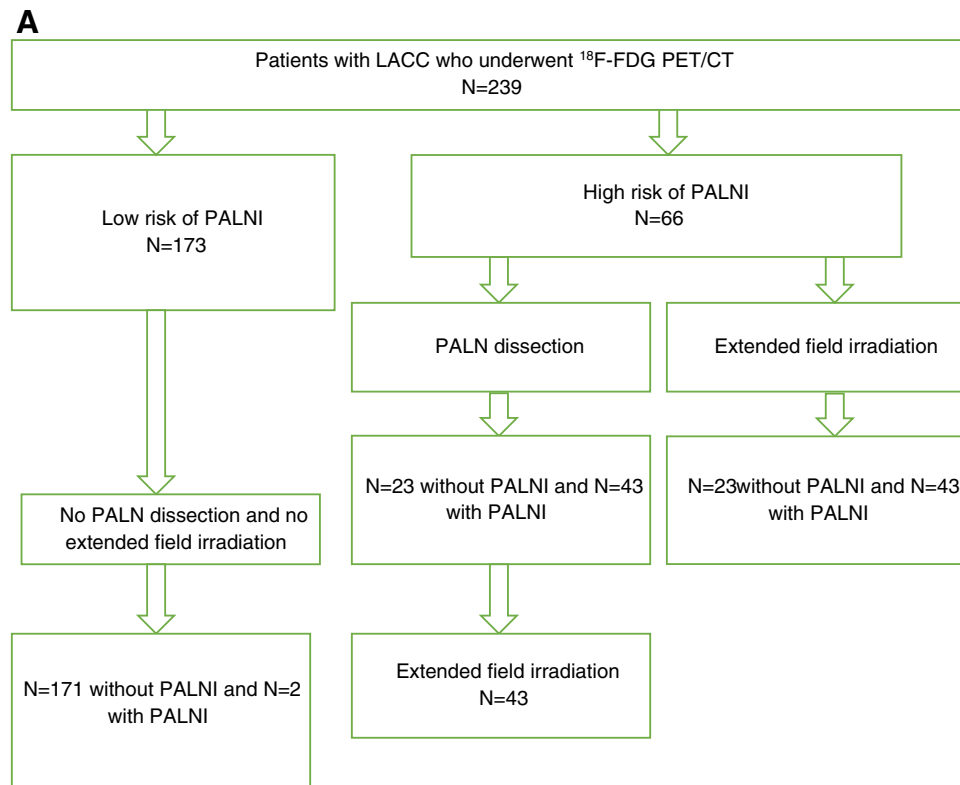


Fig. 3 Flow diagram of risk-stratification strategy based on pretreatment ^{18}F -FDG PET/CT illustrated in the pooled set after ComBat harmonization for radiomics (A) and combined models (B). The first step separates patients into two groups: low and high risk of para-aortic lymph node involvement. Low-risk group would be spared of a surgical staging and an extended field irradiation. Thus, unnecessary surgical staging would be avoided in 171 (A) or 141 (B) patients but 2 (A) or 1 (B) patient with para-aortic lymph node involvement

(PALNI) would not be treated. High-risk patients could have (i) a surgical staging followed by extended field radiotherapy in case of PALNI ii) or an extended field irradiation without surgical staging. However, 23 or 53 patients would have an unnecessary treatment. In total, 2 (A) or 1 (B) patients would not have treatment at the para-aortic level although they would have needed it but 171 (A) or 141 (B) patients would be spared of unnecessary treatment

models based on 2 radiomic features, possibly associated with the FIGO 2018 stage before surgical staging.

Many radiomic studies have focused on the prediction of pelvic LNI in early-stage cervical cancer [11–13, 15]; however, to the best of our knowledge, the present study is the first radiomic study about the prediction of PALNI in LACC. A retrospective study of 125 patients with LACC and negative PALN uptake on initial ^{18}F -FDG PET/CT who underwent para-aortic surgical dissection showed that metabolic parameters of the tumor and of the largest pelvic adenopathy in case of involvement, could help predict the risk of PALNI. The most reliable variable was the pelvic lymph node $\text{SUV}_{\text{max}}/\text{Tumor SUV}_{\text{max}}$ ratio with an AUC of 0.85. However, this was a single-center study without proper training and testing evaluation [28]. Moreover, the small volume of pelvic lymph nodes hinders an accurate and robust extraction of radiomic features. Finally, this is the first study to show the applicability of radiomics-based models from analog PET/CT to digital PET/CT. Indeed, the development of digital PET/CT to improve diagnostic accuracy but also

to reduce the radiation dose and scan time makes it necessary to validate radiomic models on this new generation of PET/CT.

In our study, we used the ComBat harmonization method which improved the performance of our models. Indeed, the use of the ComBat method is an efficient way of addressing this issue with retrospectively collected images because it only requires features extracted from patient data acquired in different departments, without requiring any phantom experiment [23]. A recent study showed that ComBat harmonization improved the performance of radiomics models but more importantly that the improvement was matrix specific [29]. This is also shown in our results where the predictive value of the GLDZM matrix features was significantly improved compared to the NGLDM matrix features.

In our study, no radiomics parameters extracted from the ADC map was significant. This result could be explained by the different b-values used for the ADC maps [30]. The two radiomic features retained in the best models are extracted from ^{18}F -FDG PET/CT. The most important,

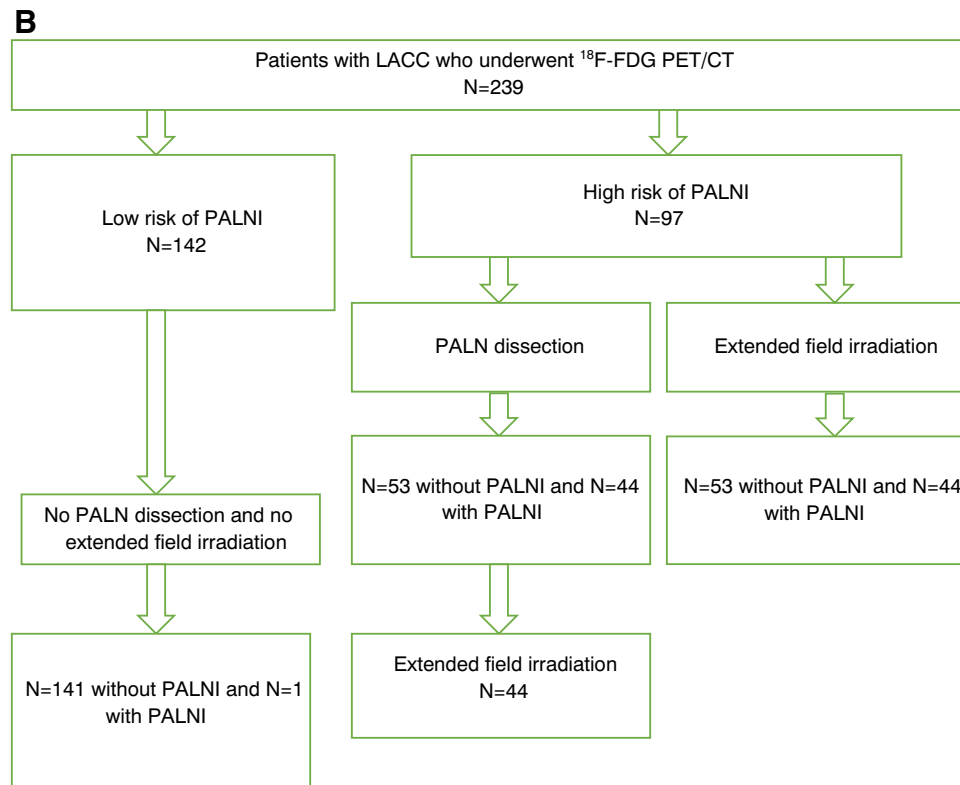


Fig. 3 (continued)

Fig. 4 Flow diagram of risk-stratification strategy based on pretreatment ^{18}F -FDG PET/CT illustrated in the squamous cell carcinoma of the CHU of Brest cohort for comparison between FRANCOGYN score (A) and radiomics (B) and combined models (C) after ComBat harmonization. The first step separates patients into two groups: low and high risk of para-aortic lymph node involvement. Low-risk group would be spared of a surgical staging and an extended field irradiation. High-risk group could have (i) a surgical staging followed by extended field radiotherapy in case of PALNI (ii) or an extended field irradiation without surgical staging. In total, compared to the FRANCOGYN score, our models spare surgical staging (55 or 54 vs 25) and avoid under-treatment of a larger number of patients (1 vs 5)

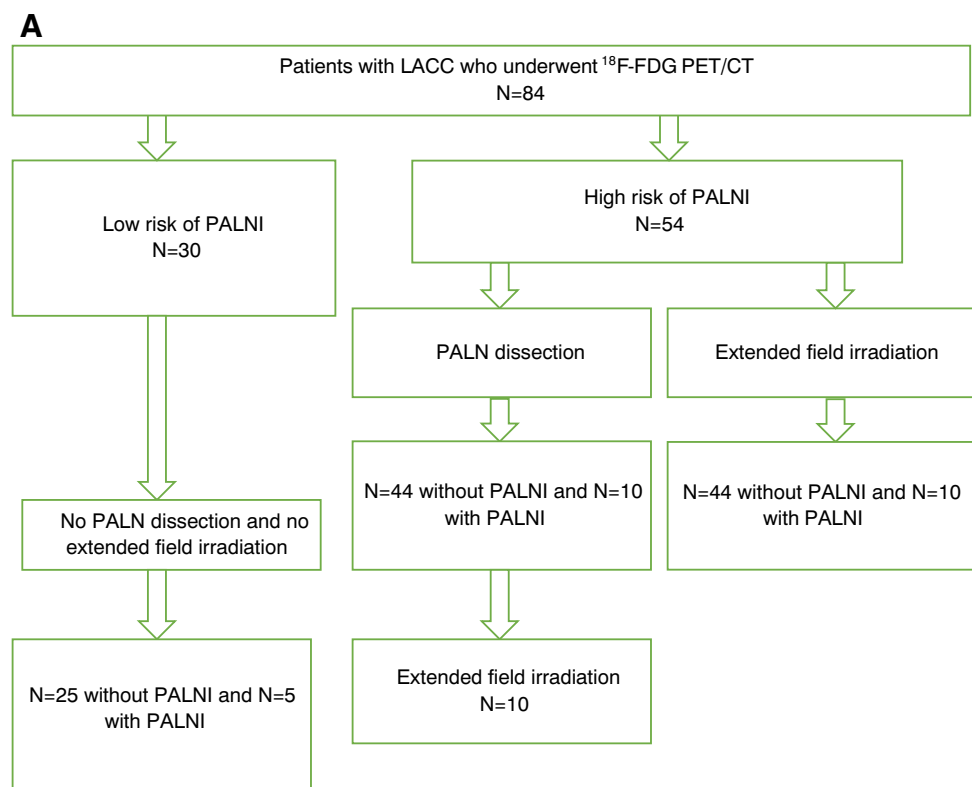


Fig. 4 (continued)

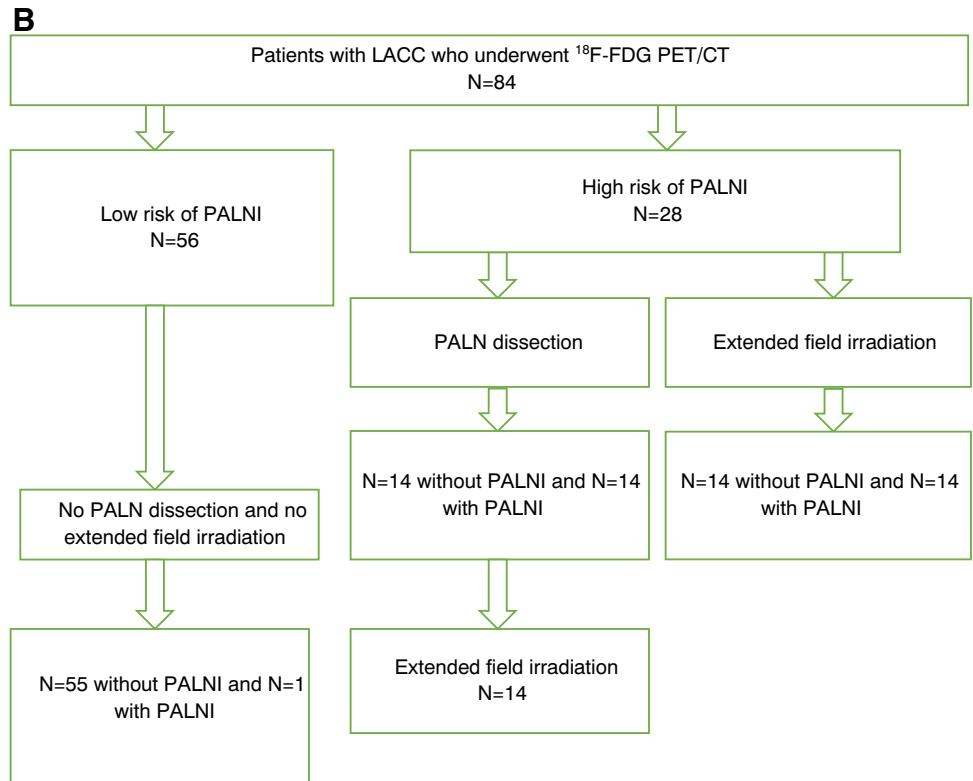
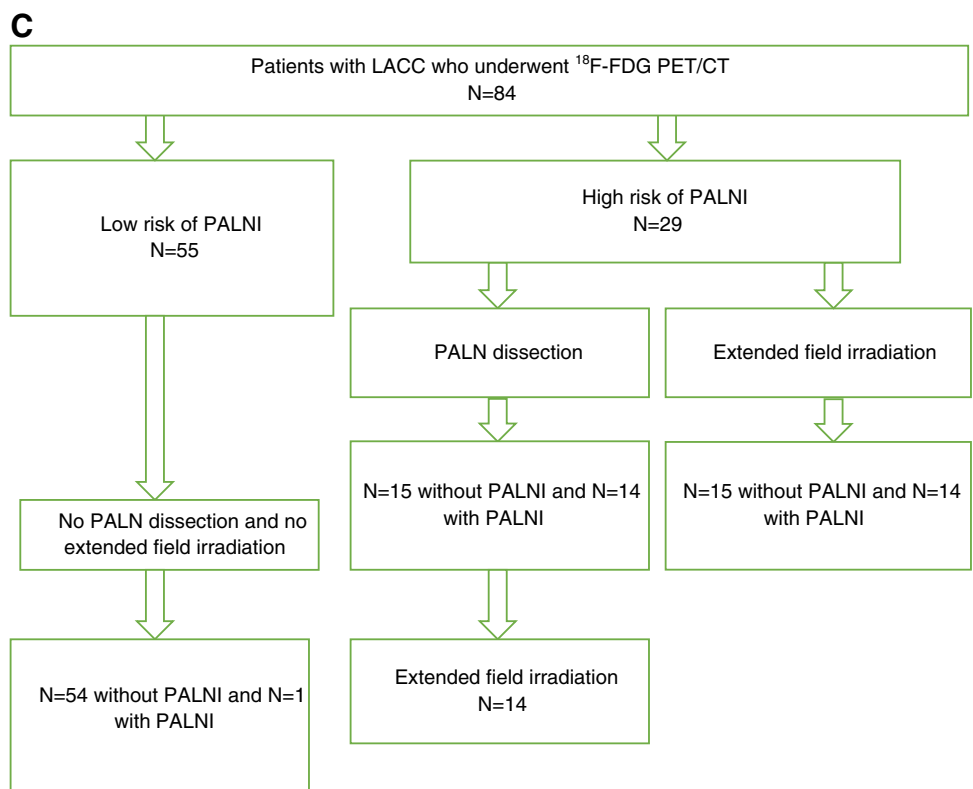


Fig. 4 (continued)



GLDZM_HISDE_PET_FBN64 (implied in 72.4% and 66.6% in the ComBat-radiomic and in the ComBat-combined models, respectively), is a textural feature which classifies heterogeneous tumors as the most likely to develop PALNI. This feature has a significant correlation ($(\rho)=0.83$) with a parameter highlighted in a previous study on the prediction of recurrence-free survival in LACC, GLDZM_DZNN_FBW0.5 [10]. It seems consistent that the risk of PALNI and recurrence-free survival are related in view of the prognostic impact of LNI. These results emphasize on the added value of radiomic features in the evaluation of tumor heterogeneity. The other one is a shape feature (Shape_maxDiameter2D3_PET_FBW0.25 is the maximum diameter is the largest pairwise difference between voxels on the surface of the volume in all coronal plans) which has a moderate correlation with the tumor size on MRI ($(\rho)=0.52$).

Our study has several limitations. The number of patients was limited with few events, which could explain the poorer results on the models built on the cohorts independently. However, the feature selection step allows to limit the bias of testing multiple features.

Its retrospective nature can lead to several biases. First, on the quality and type of nodal surgical staging (trans- vs extraperitoneal) performed. However, the 3 centers collaborating in our study are reference centers in pelvic gynecological oncology. Similarly, the likelihood of variability of the pathological examination from one center to another and its impact on the results observed is limited by the expert status of the participating centers and their compliance with international recommendations. Neural networks are sometimes perceived as “black boxes” impervious to human understanding [31]. However, in our 2 most accurate models, only 2 radiomics features are retained and their respective contributions are made available, which makes the model both explainable and interpretable. Another issue with the use of neural networks is the need to normalize the features before building the models. Indeed, since ranges of features are very different, high-value features could affect the classifier performances more than low-value features [32]. In our study, we obtained models with same performances, only the importance of the features and the cut-offs are slightly different (Supplemental data G). One reason for the identical results observed could be that very few features are included in our models. Another important question in radiomic studies is the correlation of radiomics features with standard metrics (such as SUV measurements or metabolic volume) especially in PET. One of the most important confounding factors in radiomics studies is the volume (i.e., the number of voxels). For PET radiomics specifically, textural features are unlikely to provide complementary information with respect to volume for the smallest lesions, due to the combination of the limited spatial resolution of PET imaging with the large

voxel size sampling, leading to a small number of voxels to perform texture analysis. Recent studies have shown that the lower limit actually varies depending on the feature and the methodological choices for its calculation, such as the grey-levels discretization method or the texture matrices design, suggesting a lower limit around 5 to 10 cm³ instead, although this may not be applicable to all cases [31, 33]. In our study, the range of considered volumes was 8–155 cm³ with rather large mean and median values of 42 and 28 cm³ respectively, which corresponds to 1000 voxels for the smallest volume but a mean and median number of 5250 and 3500 voxels respectively. Finally, we included a posteriori the patients from the CHU of Brest with digital PET/CT in order to validate our best radiomics-based models, without recovering the MRI images. Indeed, no radiomics features from MRI sequences were retained in the best models.

Moreover, in the case of building a model on a digital PET/CT cohort, better results can be expected because there would likely be less variability in the acquisition parameters than between analog and digital PET/CT. However, ComBat harmonization minimized this bias in our study, so it would be interesting to compare these 2 approaches when digital PET/CT becomes more broadly used and the data are sufficiently important.

Despite these limitations, our study scores 53% (19 out of 36 items) on the radiomic quality score (Supplemental data E), which compares favorably to the majority of previous radiomics studies and follows TRIPOD guidelines (Supplemental data F) [34].

Conclusion

Radiomics features extracted from pre-CRT ¹⁸F-FDG PET/CT could outperform clinical variables in the decision to individualize the indication of PALN surgical staging prior to prescription of an extended field of irradiation to PALN. This is the first study to show the applicability of radiomics-based models from analog PET/CT to digital PET/CT. Prospective validation is necessary.

Supplementary Information The online version contains supplementary material available at <https://doi.org/10.1007/s00259-023-06180-w>.

Authors' contributions All authors contributed to the study conception and design. Material preparation, data collection, and analysis were performed by François Lucia, Vincent Bourbonne, Clémence Pleyers, Mathieu Hatt, Roland Hustinx, and Pierre Lovinfosse. The first draft of the manuscript was written by François Lucia and Pierre Lovinfosse and all authors commented on previous versions of the manuscript. All authors read and approved the final manuscript.

Funding The authors declare that no funds, grants, or other support were received during the preparation of this manuscript.

Data availability The datasets generated during and/or analyzed during the current study are available from the corresponding author on reasonable request.

Declarations

Ethics approval All procedures were performed in accordance with the principles of the 1964 Declaration of Helsinki and its later amendments or comparable ethical standards. The study design and exemption from informed consent were approved by the Institutional Review Board of Liege University Hospital.

Consent to participate The study design and exemption from informed consent were approved by the Institutional Review Board of Liege University Hospital.

Competing interests The authors declare that they have no competing interests.

References


- Cibula D, Pötter R, Planchamp F, Avall-Lundqvist E, Fischerova D, Haie Meder C, et al. The European Society of Gynaecological Oncology/European Society for Radiotherapy and Oncology/European Society of Pathology guidelines for the management of patients with cervical cancer. *Radiother Oncol.* 2018;127:404–16.
- Frumovitz M, Querleu D, Gil-Moreno A, Morice P, Jhingran A, Munsell MF, et al. Lymphadenectomy in locally advanced cervical cancer study (LiLACS): Phase III clinical trial comparing surgical with radiologic staging in patients with stages IB2-IVA cervical cancer. *J Minim Invasive Gynecol.* 2014;21:3–8.
- Thelissen AAB, Jürgenliemk-Schulz IM, van der Leij F, Peters M, Gerestein CG, Zweemer RP, et al. Upstaging by para-aortic lymph node dissection in patients with locally advanced cervical cancer: a systematic review and meta-analysis. *Gynecol Oncol.* 2022;164:667–74.
- Gouy S, Morice P, Narducci F, Uzan C, Gilmore J, Kolesnikov-Gauthier H, et al. Nodal-staging surgery for locally advanced cervical cancer in the era of PET. *Lancet Oncol.* 2012;13:e212–220.
- Cibula D, Borčinová M, Marnitz S, Jarkovský J, Klát J, Pilka R, et al. Lower-limb lymphedema after sentinel lymph node biopsy in cervical cancer patients. *Cancers (Basel).* 2021;13:2360.
- Nasioudis D, Rush M, Taunk NK, Ko EM, Haggerty AF, Cory L, et al. Oncologic outcomes of surgical para-aortic lymph node staging in patients with advanced cervical carcinoma undergoing chemoradiation. *Int J Gynecol Cancer.* 2022;32:823–7.
- Dabi Y, Simon V, Carcopino X, Bendifallah S, Ouldamer L, Lavoue V, et al. Therapeutic value of surgical paraaortic staging in locally advanced cervical cancer: a multicenter cohort analysis from the FRANCOGYN study group. *J Transl Med.* 2018;16:326.
- Nguyen-Xuan HT, Benoit L, Dabi Y, Touboul C, Raimond E, Ballester M, et al. How to predict para-aortic node involvement in advanced cervical cancer? Development of a predictive score. A FRANCOGYN study. *Eur J Surg Oncol.* 2021;47:2900–6.
- Lucia F, Visvikis D, Vallières M, Desseroit M-C, Miranda O, Robin P, et al. External validation of a combined PET and MRI radiomics model for prediction of recurrence in cervical cancer patients treated with chemoradiotherapy. *Eur J Nucl Med Mol Imaging.* 2019;46:864–77.
- Ferreira M, Lovinfosse P, Hermesse J, Decuyper M, Rousseau C, Lucia F, et al. [18F]FDG PET radiomics to predict disease-free survival in cervical cancer: a multi-scanner/center study with external validation. *Eur J Nucl Med Mol Imaging.* 2021;48:3432–43.
- Li K, Sun H, Lu Z, Xin J, Zhang L, Guo Y, et al. Value of [18F] FDG PET radiomic features and VEGF expression in predicting pelvic lymphatic metastasis and their potential relationship in early-stage cervical squamous cell carcinoma. *Eur J Radiol.* 2018;106:160–6.
- Li L, Zhang J, Zhe X, Tang M, Zhang X, Lei X, et al. A meta-analysis of MRI-based radiomic features for predicting lymph node metastasis in patients with cervical cancer. *Eur J Radiol.* 2022;151: 110243.
- Li X-R, Jin J-J, Yu Y, Wang X-H, Guo Y, Sun H-Z. PET-CT radiomics by integrating primary tumor and peritumoral areas predicts E-cadherin expression and correlates with pelvic lymph node metastasis in early-stage cervical cancer. *Eur Radiol.* 2021;31:5967–79.
- Dong T, Yang C, Cui B, Zhang T, Sun X, Song K, et al. Development and validation of a deep learning radiomics model predicting lymph node status in operable cervical cancer. *Front Oncol.* 2020;10:464.
- Chen J, He B, Dong D, Liu P, Duan H, Li W, et al. Noninvasive CT radiomic model for preoperative prediction of lymph node metastasis in early cervical carcinoma. *Br J Radiol.* 2020;93:20190558.
- Yasaka K, Akai H, Abe O, Kiryu S. Deep learning with convolutional neural network for differentiation of liver masses at dynamic contrast-enhanced CT: a preliminary study. *Radiology.* 2018;286:887–96.
- Opitz D, Maclin R. Popular ensemble methods: an empirical study. *jair.* 1999;11:169–98.
- Bourbonne V, Lucia F, Jaouen V, Bert J, Rehn M, Pradier O, et al. Development and prospective validation of a spatial dose pattern based model predicting acute pulmonary toxicity in patients treated with volumetric arc-therapy for locally advanced lung cancer. *Radiother Oncol.* 2021;164:43–9.
- Delcroix O, Bourhis D, Keromnes N, Robin P, Le Roux P-Y, Abgral R, et al. Assessment of image quality and lesion detectability with digital PET/CT system. *Front Med (Lausanne).* 2021;8: 629096.
- Belli ML, Mori M, Broggi S, Cattaneo GM, Bettinardi V, Dell'Oca I, et al. Quantifying the robustness of [18F]FDG-PET/CT radiomic features with respect to tumor delineation in head and neck and pancreatic cancer patients. *Phys Med.* 2018;49:105–11.
- Velazquez ER, Parmar C, Jermoumi M, Mak RH, van Baardwijk A, Fennessy FM, et al. Volumetric CT-based segmentation of NSCLC using 3D-Slicer. *Sci Rep.* 2013;3:3529.
- Zwanenburg A, Vallières M, Abdalah MA, Aerts HJWL, Andrearczyk V, Apte A, et al. The image biomarker standardization initiative: standardized quantitative radiomics for high-throughput image-based phenotyping. *Radiology.* 2020;295:328–38.
- Fortin J-P, Cullen N, Sheline YI, Taylor WD, Aselcioglu I, Cook PA, et al. Harmonization of cortical thickness measurements across scanners and sites. *Neuroimage.* 2018;167:104–20.
- Gouy S, Morice P, Narducci F, Uzan C, Martinez A, Rey A, et al. Prospective multicenter study evaluating the survival of patients with locally advanced cervical cancer undergoing laparoscopic para-aortic lymphadenectomy before chemoradiotherapy in the era of positron emission tomography imaging. *J Clin Oncol.* 2013;31:3026–33.
- De Cuypere M, Lovinfosse P, Goffin F, Gennigens C, Rovira R, Duch J, et al. Added value of para-aortic surgical staging compared to 18F-FDG PET/CT on the external beam radiation field for patients with locally advanced cervical cancer: an ONCO-GF study. *Eur J Surg Oncol.* 2020;46:883–7.
- Gouy S, Seebacher V, Chargari C, Terroir M, Grimaldi S, Ilenko A, et al. False negative rate at 18F-FDG PET/CT in para-aortic

- lymphnode involvement in patients with locally advanced cervical cancer: impact of PET technology. *BMC Cancer*. 2021;21:135.
27. Smits RM, Zusterzeel PLM, Bekkers RLM. Pretreatment retroperitoneal para-aortic lymph node staging in advanced cervical cancer: a review. *Int J Gynecol Cancer*. 2014;24:973–83.
 28. Martinez A, Voglimacci M, Lusque A, Ducassou A, Gladieff L, Dupuis N, et al. Tumour and pelvic lymph node metabolic activity on FDG-PET/CT to stratify patients for para-aortic surgical staging in locally advanced cervical cancer. *Eur J Nucl Med Mol Imaging*. 2020;47:1252–60.
 29. Leithner D, Schöder H, Haug A, Vargas HA, Gibbs P, Häggström I, et al. Impact of ComBat harmonization on PET radiomics-based tissue classification: a dual-center PET/MRI and PET/CT Study. *J Nucl Med*. 2022;63:1611–6.
 30. Becker AS, Wagner MW, Wurnig MC, Boss A. Diffusion-weighted imaging of the abdomen: impact of b-values on texture analysis features. *NMR Biomed*. 2017;30(1). <https://doi.org/10.1002/nbm.3669>.
 31. Hatt M, Cheze Le Rest C, Antonorsi N, Tixier F, Tankyevych O, Jaouen V, et al. Radiomics in PET/CT: current status and future AI-based evolutions. *Semin Nucl Med*. 2021;51:126–33.
 32. Duda RO, Hart EP, Stork DG. Pattern classification. 2nd ed. 1973. https://www.researchgate.net/publication/228058014_Pattern_Classification.
 33. Hatt M, Tixier F, Pierce L, Kinahan PE, Le Rest CC, Visvikis D. Characterization of PET/CT images using texture analysis: the past, the present... any future? *Eur J Nucl Med Mol Imaging*. 2017;44:151–65.
 34. Heus P, Damen JAAG, Pajouheshnia R, Scholten RJPM, Reitsma JB, Collins GS, et al. Uniformity in measuring adherence to reporting guidelines: the example of TRIPOD for assessing completeness of reporting of prediction model studies. *BMJ Open*. 2019;9: e025611.

Publisher's note Springer Nature remains neutral with regard to jurisdictional claims in published maps and institutional affiliations.

Springer Nature or its licensor (e.g. a society or other partner) holds exclusive rights to this article under a publishing agreement with the author(s) or other rightsholder(s); author self-archiving of the accepted manuscript version of this article is solely governed by the terms of such publishing agreement and applicable law.

Authors and Affiliations

François Lucia^{1,2,3}  · Vincent Bourbonne^{1,2} · Clémence Pleyers⁴ · Pierre-François Dupré⁵ · Omar Miranda¹ · Dimitris Visvikis² · Olivier Pradier^{1,2} · Ronan Abgral^{6,7} · Augustin Mervoyer⁸ · Jean-Marc Classe⁹ · Caroline Rousseau^{10,11} · Wim Vos¹² · Johanne Hermesse⁴ · Christine Gennigens¹³ · Marjolein De Cuypere¹⁴ · Frédéric Kridelka¹⁴ · Ulrike Schick^{1,2} · Mathieu Hatt² · Roland Hustinx³ · Pierre Lovinfosse³

¹ Radiation Oncology Department, University Hospital, Brest, France

² LaTIM, INSERM, UMR 1101, Univ Brest, Brest, France

³ Division of Nuclear Medicine and Oncological Imaging, University Hospital of Liège, Liège, Belgium

⁴ Department of Radiotherapy Oncology, University Hospital of Liège, Liège, Belgium

⁵ Department of Gynecology and Surgery, University Hospital, Brest, France

⁶ Nuclear Medicine Department, University Hospital, Brest, France

⁷ EA GETBO 3878, IFR 148, University of Brest, UBO, Brest, France

⁸ Department of Radiation Oncology, Institut de Cancérologie de l'Ouest Centre René Gauducheau, Saint Herblain, France

⁹ Department of Surgical Oncology, Institut de Cancérologie de l'Ouest Centre René Gauducheau, Saint Herblain, France

¹⁰ Université de Nantes, CNRS, Inserm, CRCINA, F-44000 Nantes, France

¹¹ ICO René Gauducheau, F-44800 Saint-Herblain, France

¹² Radiomics SA, Liège, Belgium

¹³ Department of Medical Oncology, University Hospital of Liège, Liège, Belgium

¹⁴ Department of Gynecology, University Hospital of Liège, Liège, Belgium